Fluid Phase Equilibria 418 (2016) 160–174

Contents lists available at ScienceDirect

Fluid Phase Equilibria

journal homepage: www.elsevier.com/locate/fluid

Thermodynamic modeling of aqueous systems containing amines and amine hydrochlorides: Application to methylamine, morpholine, and morpholine derivatives

Malgorzata M. Lencka, Jerzy J. Kosinski, Peiming Wang, Andrzej Anderko*

OLI Systems Inc., 240 Cedar Knolls Road, Suite 301, Cedar Knolls, NJ, 07927, USA

ARTICLE INFO

Article history:
Received 29 August 2015
Received in revised form
12 October 2015
Accepted 14 October 2015
Available online 17 October 2015

Keywords:
Amines
Amine hydrochlorides
Electrolyte modeling
Aqueous speciation
Solid–liquid–vapor equilibria

ABSTRACT

A comprehensive thermodynamic model has been developed for calculating phase equilibria and speciation in aqueous mixtures containing neutralizing amines and corresponding amine hydrochlorides. The model has been designed to simulate the behavior of refinery overhead environments, in which the presence of amines in combination with hydrogen chloride may lead to the formation of potentially corrosive solid or concentrated aqueous amine hydrochloride phases. For this purpose, the previously developed Mixed-Solvent Electrolyte (MSE) model has been extended to calculate simultaneously solid–gas, solid–liquid, and vapor–liquid equilibria, liquid-phase chemical equilibria, and caloric properties. In the model, standard-state properties of individual species are calculated from the Helgeson–Kirkham–Flowers equation of state whereas the excess Gibbs energy includes a long-range electrostatic interaction term expressed by a Pitzer–Debye–Hückel equation, a virial coefficient-type term for interactions between ions and a short-range term for interactions involving neutral molecules. This framework accurately represents the properties of systems that range from weak electrolytes, such as amine – water mixtures, to strong electrolytes such as amine hydrochloride – water solutions. For amine hydrochlorides, the model is applicable up to the limit of solid or fused liquid hydrochloride phases. Model parameters have been developed for methylamine, morpholine, N-methylmorpholine, N-ethylmorpholine and their hydrochlorides. The model offers the possibility of understanding the formation of amine hydrochlorides in multicomponent mixtures containing amines, water, hydrogen chloride, and carbon dioxide.

1. Introduction

Neutralizing amines are commonly used in many industrial applications to control corrosion. In particular, prominent applications include mitigating corrosion in refinery overhead systems [1–6] and in nuclear power plants [7–12]. In refining, various amines are added to neutralize hydrogen chloride, which results from the hydrolysis of alkaline earth chlorides that are found in crude oil. However, while the injection of amines reduces the risk of acid corrosion, it may lead to the formation of amine hydrochloride salts. Amine hydrochlorides may form either solid or concentrated aqueous phases, which may cause aggressive corrosion in refinery overheads. Thus, it is important to understand and to be able to predict the conditions that lead to such phenomena. Because of the inherent difficulties in monitoring the phase behavior in actual refinery settings, a thermodynamic model that can realistically predict these phenomena can be of great value. However, the development of such a model is very challenging because refinery overhead systems are complex mixtures of hydrocarbons, water, acid gases, and amines.

A tremendous amount of research has been devoted in the literature to the thermodynamic behavior of amine systems that are used for CO_2 capture and acid gas removal applications. Much less work has been published on the behavior of amines in the context of corrosion control in refining. Although there is a substantial overlap in the amine mixture properties that are required for acid gas removal and for corrosion control, the fundamental difference lies in the fact that refinery corrosion control is inextricably linked with the presence of hydrogen chloride, which induces the formation of amine hydrochlorides. Thus, this study is focused

* Corresponding author.
E-mail address: aanderko@olisystems.com (A. Anderko).

http://dx.doi.org/10.1016/j.fluid.2015.10.025
0378-3812/

on the properties of amine hydrochlorides as well as on those of the underlying amines.

The neutralizing amines that are used in the refining industry include primary alkyl amines (e.g., methylamine, ethylamine, propylamine, butylamine, cyclohexylamine, etc.), secondary alkyl amines (e.g., dimethylamine or diethylamine), tertiary alkyl amines (e.g., trimethylamine), alkoxy amines (e.g., 3-methoxypropylamine), cyclic ether amines (e.g., morpholine, N-methylmorpholine, N-ethylmorpholine, etc.), and alkanolamines (e.g., ethanolamine, diethanolamine, methyldiethanolamine, dimethylethanolamine, dimethylisopropanolamine, diglycolamine, etc.) Because of the differences in their molecular structure, these amines differ with respect to their volatility and their phase equilibria with water and hydrocarbons. Thus, their partitioning between the gas phase, hydrocarbon-rich liquid phase and aqueous phase differs widely. Also, the amines differ with respect to their propensity to form solid amine hydrochlorides or concentrated aqueous solutions containing amine hydrochlorides in an ionic form. Frequently, mixtures of amines are used, which additionally complicates the prediction of their behavior in refinery environments. Among the neutralizing amines, selected alkanolamines have been studied in great detail in the literature in conjunction with acid gas removal and CO_2 capture applications. In general, the other families of amines have been studied to a lesser extent.

In order to predict the possibility of corrosion in refinery overheads, it is necessary to construct a thermodynamic model for multicomponent mixtures that include water, amines, amine hydrochlorides, hydrogen chloride, carbon dioxide, and hydrocarbons. In general, such mixtures may form multiphase systems, including a gas phase, a hydrocarbon-rich liquid phase, an aqueous phase and solid amine hydrochloride phases. A conceptual scheme of the phases, species, and phase equilibria in such systems is shown in Fig. 1. In this figure, the amines are denoted as RNH_2 for simplicity. Thus, a comprehensive model must simultaneously reproduce:

(i) Vapor–liquid equilibria for mixtures of amines with water, which is necessary to predict the partitioning of amines between the vapor and aqueous phases;
(ii) Vapor–solid equilibria for amine hydrochlorides, which determines the possibility of precipitation of amine hydrochlorides from the gas phase;

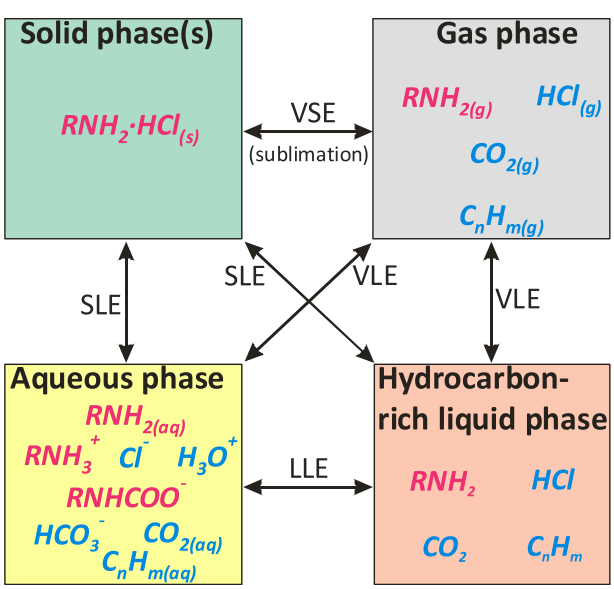

Fig. 1. A conceptual scheme of the phases, species, and phase equilibria that may appear in conjunction with the application of neutralizing amines.

(iii) Solid–liquid and solid–liquid–vapor equilibria for amine hydrochlorides in water, which influence the transition between solid amine hydrochlorides and concentrated amine hydrochloride solutions, the latter being of particular interest for predicting conditions that are conducive to corrosion;
(iv) Speciation in the aqueous phase involving the equilibrium between molecular and ionized forms of the amines, dissociation of acid gases and formation of carbamate ions in the presence of CO_2;
(v) Partitioning of amines and acid gases between the gas phase and the hydrocarbon-rich liquid phase, which influences the availability of the amines and HCl in the aqueous phase.

Also, it should be noted that substantial overlap exists between the neutralizing amines used in refinery overheads and those used for water treatment in nuclear steam generating systems. In the latter case, the phase behavior and speciation at high temperatures are of particular interest while the formation of amine hydrochlorides is not expected. Thus, it is possible to develop a model that simultaneously addresses the refinery overhead and power plant conditions.

In order to develop a thermodynamic model that satisfies conditions (i-v), we extend the previously developed Mixed-Solvent Electrolyte (MSE) computational framework of Wang et al. [13–15]. This framework was designed for the simultaneous calculation of phase and chemical equilibria in systems containing strong and weak electrolytes in aqueous, non-aqueous and mixed solvents. In particular, it was shown to be applicable to electrolyte solutions up to the fused salt limit [13] and to reproduce acid-base equilibria in environments dominated either by water or by other protic solvents [16,17]. Furthermore, it was applied to systems containing acid gases in wide temperature and pressure ranges [18,19], salt solutions with complex solid–liquid–vapor equilibria [20] and ionic liquid mixtures [21]. However, the amine hydrochlorides that are of interest here constitute a somewhat different class of systems for thermodynamic modeling. On the one hand, they form strong electrolytes. On the other hand, they have relatively low melting points and are much more volatile than the majority of salts or ionic liquids. Thus, the model needs to reproduce vapor–solid as well as vapor–liquid and vapor–liquid–solid equilibria in systems containing amine hydrochlorides.

In this study, we focus on phase and chemical equilibria in mixtures containing water, amines and their corresponding hydrochlorides, HCl, and CO_2. The behavior of amine – hydrocarbon mixtures (especially the partitioning of amines between aqueous and hydrocarbon phases) requires a separate study. The amines that have been selected for this study include methylamine and three cyclic ether amines, i.e., morpholine, N-methylmorpholine, and N-ethylmorpholine. These amines represent primary (methylamine), secondary (morpholine) and tertiary (N-methyl- and N-ethylmorpholines) amines and span a relatively wide range of volatilities. The available experimental data are analyzed and a comprehensive set of parameters is developed to model the thermodynamic behavior of vapor – liquid – solid mixtures that can range from weak electrolyte systems, such as the amine – water – CO_2 mixtures, to strong, yet volatile electrolyte solutions containing amine hydrochlorides.

2. Thermodynamic model

2.1. Solution speciation and phase equilibria

To model the behavior of both amines and amine hydrochlorides, the hydrolysis (or protonation) of the amine is of key importance. For methylamine, the hydrolysis reaction can be written as

$$CH_3NH_{2(aq)} + H_2O = CH_3NH_3^+ + OH^- \quad (1)$$

For morpholine and its N-methyl and N-ethyl derivatives, analogous reactions are given as

$$O(CH_2CH_2)_2NR_{(aq)} + H_2O = O(CH_2CH_2)_2NRH^+ + OH^- \quad (2)$$

where R represents H for morpholine, CH_3 for N-methylmorpholine and C_2H_5 for N-ethylmorpholine. Further, primary and secondary amines undergo reactions with carbon dioxide that lead to the formation of carbamate ions. In the case of morpholine, the carbamate formation reaction is

$$O(CH_2CH_2)_2NH_{(aq)} + HCO_3^- = O(CH_2CH_2)_2NCOO^- + H_2O \quad (3)$$

These amine speciation reactions are considered in conjunction with the self-dissociation of water, i.e.,

$$2H_2O = H_3O^+ + OH^- \quad (4)$$

and with the dissociation of dissolved acid gases, i.e., HCl and CO_2:

$$HCl_{(aq)} + H_2O = H_3O^+ + Cl^- \quad (5)$$

$$CO_{2(aq)} + 2H_2O = H_3O^+ + HCO_3^- \quad (6)$$

$$HCO_3^- + H_2O = H_3O^+ + CO_3^{2-} \quad (7)$$

Solid amine hydrochlorides may form as a result of gas-phase reactions between an amine and HCl. Thus, for methylamine hydrochloride, the solid–vapor equilibrium is defined as

$$CH_3NH_2 \cdot HCl_{(s)} = CH_3NH_{2(g)} + HCl_{(g)} \quad (8)$$

and for morpholine and its derivatives it is written as

$$O(CH_2CH_2)_2NR \cdot HCl_{(s)} = O(CH_2CH_2)_2NR_{(g)} + HCl_{(g)} \quad (9)$$

In the presence of a liquid phase, amine hydrochlorides may also undergo solid–liquid equilibria, i.e.,

$$CH_3NH_2 \cdot HCl_{(s)} = CH_3NH_3^+ + Cl^- \quad (10)$$

for methylamine hydrochloride and

$$O(CH_2CH_2)_2NR \cdot HCl_{(s)} = O(CH_2CH_2)_2NRH^+ + Cl^- \quad (11)$$

for the hydrochlorides of morpholine and its derivatives. It has been assumed that the amine-H^+ and Cl^- ions do not form ion pairs in the aqueous phase. Although this assumption may be questioned, there is a lack of thermodynamic information on amine hydrochloride ion pairing.

The equilibrium state of the system is obtained by solving the equilibrium expressions for reactions (1)–(11) coupled with vapor–liquid equilibrium conditions. By rewriting Eqs. (1)–(11) in the generic form

$$\sum \nu_i A_i = 0, \quad (12)$$

where ν_i are the stoichiometric coefficients and A_i are the species, the equilibrium condition is given by

$$\sum \nu_i \mu_i = 0 \quad (13)$$

where μ_i is the chemical potential of species i. The vapor–liquid equilibrium condition is computed for all species that can exist in the gas phase, i.e., the neutral forms of the amines, HCl, CO_2, and H_2O:

$$\mu_i^L = \mu_i^G \quad (14)$$

Eqs. (13) and (14) are solved together with material balance and electroneutrality constraints as described by Zemaitis et al. [22] and Rafal et al. [23] For this purpose, the chemical potentials are calculated using the MSE model.

2.2. Mixed-solvent electrolyte model

The Mixed-Solvent Electrolyte (MSE) thermodynamic framework was described in detail in previous studies [13–15]. Here, we summarize the key elements of the model in order to define the parameters that need to be evaluated to reproduce both chemical and phase equilibria in systems containing amines and amine hydrochlorides.

In the MSE model, the chemical potential of a species i in the liquid phase is calculated as

$$\mu_i^L = \mu_i^{L,0,x}(T,P) + RT \ln x_i \gamma_i^{x,*}(T,P,\mathbf{x}) \quad (15)$$

where $\mu_i^{L,0,x}(T,P)$ is the standard-state chemical potential expressed on the mole fraction basis, x_i is the mole fraction, and $\gamma_i^{x,*}(T,P,\mathbf{x})$ is the unsymmetrically normalized, mole fraction-based activity coefficient of species i. The mole fraction-based standard-state chemical potential is related to the more frequently used molality-based standard-state chemical potential by Ref. [13]:

$$\mu_i^{L,0,x}(T,P) = \mu_i^{L,0,m}(T,P) + RT \ln \frac{1000}{M_{H_2O}} \quad (16)$$

where M_{H_2O} is the molecular weight of water. The molality-based standard-state chemical potential is calculated as a function of temperature and pressure from the Helgeson–Kirkham–Flowers (HKF) equation of state [24–27]. The HKF model accurately reproduces thermodynamic properties of species (and, hence, the equilibrium constants for reactions between them) up to 1000 °C and 5 kbar. For water, the standard-state chemical potential is defined as that of pure water and is calculated from the Haar–Gallagher–Kell equation of state [28].

The activity coefficients in Eq. (15) are obtained from an expression for the excess Gibbs energy, which is constructed as a sum of three contributions:

$$G^{ex} = G_{LR}^{ex} + G_{II}^{ex} + G_{SR}^{ex} \quad (17)$$

where G_{LR}^{ex} is the contribution of long-range electrostatic interactions, G_{II}^{ex} represents ionic (ion–ion and ion–molecule) interactions, and G_{SR}^{ex} accounts for a short-range contribution resulting from intermolecular interactions. The long-range interaction contribution is calculated from the Debye–Hückel theory as revised by Pitzer [29] and expressed in terms of mole fractions, *i.e.*,

$$\frac{G_{LR}^{ex}}{RT} = -\left(\sum_i n_i\right) \frac{4A_x I_x}{\rho} \ln\left(\frac{1+\rho I_x^{1/2}}{\sum_i x_i \left[1+\rho\left(I_{x,i}^0\right)^{1/2}\right]}\right) \quad (18)$$

where I_x is the mole fraction-based ionic strength, $I_{x,i}^0$ is defined as the ionic strength in the limiting case when $x_i = 1$, *i.e.*, $I_{x,i}^0 = 0.5z_i^2$; ρ is assigned a universal dimensionless value ($\rho = 14$) and A_x is given by

$$A_x = \frac{1}{3}(2\pi N_A d_s)^{1/2}\left(\frac{e^2}{4\pi\varepsilon_0\varepsilon_s k_B T}\right)^{3/2} \tag{19}$$

where d_s and ε_s are the molar density and dielectric constant of the solvent, respectively, N_A is the Avogadro constant, e is the electron charge, ε_0 is the vacuum permittivity, and k_B is the Boltzmann constant.

The ion-interaction contribution is calculated from an ionic strength-dependent, symmetrical virial-type expression [13]:

$$\frac{G_{II}^{ex}}{RT} = -\left(\sum_i n_i\right)\sum_i\sum_j x_i x_j B_{ij}(I_x) \tag{20}$$

where $B_{ij}(I_x) = B_{ji}(I_x)$, $B_{ii} = B_{jj} = 0$, and the ionic strength dependence of B_{ij} is given by

$$B_{ij}(I_x) = b_{ij} + c_{ij}\exp\left(-\sqrt{I_x + a_1}\right) \tag{21}$$

where b_{ij} and c_{ij} are binary interaction parameters and a_1 has a fixed value of 0.01. In general, the parameters b_{ij} and c_{ij} are expressed as functions of temperature and pressure [18]. For the systems studied here, no pressure dependence is required and these parameters are expressed as:

$$b_{ij} = b_{0,ij} + b_{1,ij}T + b_{2,ij}/T \tag{22}$$

$$c_{ij} = c_{0,ij} + c_{1,ij}T + c_{2,ij}/T \tag{23}$$

For most binary pairs, only a limited subset of the coefficients of Eqs. (22) and (23) needs to be used. The short-range interaction contribution is calculated from the UNIQUAC equation [30]:

$$\frac{G_{SR}^{ex}}{RT} = \left(\sum_i n_i\right)\left[\sum_i x_i \ln\frac{\phi_i}{x_i} + \frac{Z}{2}\sum_i q_i x_i \ln\frac{\theta_i}{\phi_i}\right] - \left(\sum_i n_i\right)\left[\times\sum_i q_i x_i \ln\left(\sum_j \theta_j \tau_{ij}\right)\right] \tag{24}$$

where the quantities θ_i, ϕ_i, and τ_i are defined as

$$\theta_i = \frac{q_i x_i}{\sum_j q_j x_j} \tag{25}$$

$$\phi_i = \frac{r_i x_i}{\sum_j r_j x_j} \tag{26}$$

$$\tau_{ji} = \exp\left(-\frac{a_{ji}}{RT}\right) \tag{27}$$

where q_i and r_i are the surface and size parameters, respectively, Z is a fixed coordination number ($Z = 10$), and a_{ij} ($a_{ij} \neq a_{ji}$) are binary interaction parameters. For the systems studied here, they are expressed as functions of temperature by

$$a_{ij} = a_{ij}^{(0)} + a_{ij}^{(1)}T + a_{ij}^{(2)}T^2 \tag{28}$$

For systems containing only strong electrolytes, only the ion interaction parameters (Eqs. (22)–(23)) are needed. The short-range parameters (Eq. (28)) are introduced for interactions involving neutral molecules.

The activity coefficients are calculated from Eq. (17) by differentiation with respect to the number of moles using standard thermodynamics [31]. Since the activity coefficients that are calculated directly from Eq. (20) are symmetrically normalized (i.e., they are equal to 1 for each pure component), they are then converted to unsymmetrical normalization, in which the activity coefficient of water is equal to 1 in pure water and those of all the remaining species approach 1 at infinite dilution. This conversion is made in order to utilize the activity coefficients in conjunction with the HKF equation for the standard-state properties of solute species, which are defined using the infinite-dilution reference state. The conversion is given by:

$$\ln\gamma_i^{x,*} = \ln\gamma_i^x - \lim_{\substack{x_i\to 0\\ x_w\to 1}}\ln\gamma_i^x \tag{29}$$

where $\lim_{\substack{x_i\to 0\\ x_w\to 1}}\ln\gamma_i^x$ is the value of the symmetrically-normalized activity coefficient at infinite dilution in water. The activity coefficient obtained from Eq. (29) is then used in Eq. (15).

The chemical potential of species i in the gas phase is given by the standard relation

$$\mu_i^G = \mu_i^{G,0}(T) + RT\ln\frac{Py_i\varphi_i(T,P)}{P^0} \tag{30}$$

where $\mu_i^{G,0}(T)$ is the chemical potential of pure component i in the ideal gas state, y_i is the mole fraction in the gas phase, $\varphi_i(T,P)$ is the fugacity coefficient, P is the total pressure, and $P^0 = 1$ atm. The $\mu_i^{G,0}(T)$ term is calculated from the ideal-gas Gibbs energy of formation, $\Delta G_f^{G,0}$, absolute entropy, $S^{G,0}$, and heat capacity as a function of temperature, $C_p^G(T)$, using standard thermodynamics [31]. For water, this term is obtained from the equation of state of Haar et al. [28] The fugacity coefficient is calculated from the Soave–Redlich–Kwong (SRK) equation of state [32].

The solid amine hydrochlorides are assumed to be pure phases because there is no evidence of hydrate or solid solution formation. The chemical potential of the pure solid phases, $\mu_i^{S,0}(T)$, is calculated as a function of temperature from the solid-state standard-state Gibbs energy of formation, $\Delta G_f^{S,0}$, absolute entropy,$S^{S,0}$, and heat capacity as a function of temperature, $C_p^S(T)$.

2.3. Parameterization of the model

The parameters of the MSE model have been determined by analyzing and regressing the available thermodynamic data. The sources of the data are summarized in Table A-1 in the Appendix together with their temperature ranges and their types (i.e., pure component vapor pressure of liquids and solids, heat capacity of pure liquid, solid, and ideal-gas, vapor–liquid equilibria, solid–liquid equilibria and heat capacity of mixtures, dissociation equilibria and speciation). Tables 1 through 6 provide a complete set of parameters that are necessary to reproduce the properties of the amine and amine hydrochloride systems. Specifically, Table 1 summarizes the properties of individual species at infinite dilution in water, Tables 2 and 3 list the binary parameters in the ion-interaction and short-range terms, respectively, and Tables 4–6 collect the requisite properties of individual species in the liquid, gas, and solid phases, respectively.

The parameters have been determined in a multi-step procedure. First, the parameters have been established for the binary mixtures of amines and water. Since the model uses infinite dilution in water as the reference state in the liquid phase (cf. Eq. (15)), the properties of binary mixtures need to be regressed together

with the properties of pure amines. In aqueous solutions, the amines are weak electrolytes. Therefore, in view of the low equilibrium concentration of the ionized form of the amine in amine-water mixtures, vapor–liquid equilibria are overwhelmingly determined by the properties of the neutral species and the ionized form makes an appreciable contribution only in dilute solutions. Thus, the parameters for amine – water binaries have been determined as follows:

(a) The chemical potential in the gas phase is calculated according to Eq. (30) using the ideal-gas thermochemical properties from Table 5;
(b) The liquid-phase chemical potential is constrained to reproduce the pure-liquid heat capacity, as calculated using the coefficients collected in Table 4, using a procedure described in a previous study [13];
(c) Then, the short-range interaction parameters (Eq. (28)) and the standard Gibbs energy of formation, $\Delta\overline{G}_f^0$, and entropy, $\overline{S}^0$, of the neutral amine at infinite dilution in water (which determine the standard-state chemical potential $\mu_i^{L,0,x}(T,P)$ in Eq. (15)) are simultaneously determined by regressing vapor–liquid equilibria for binary amine-water systems, pure-component vapor pressure of the amine and heat capacity data in binary systems. The r and q parameters that are used in Eqs. (25) and (26) are listed in Table 4. The obtained parameters $\Delta\overline{G}_f^0$ and $\overline{S}^0$ are collected in Table 1 and the short-range interaction parameters are listed in Table 3. The parameters $\Delta\overline{G}_f^0$ and $\overline{S}^0$ are intrinsically related to the Henry's law constant for the amine whereas the short-range interaction parameters ensure that the properties of the mixture are reproduced from infinite dilution of the amine in water to the pure amine limit.
(d) After determining the parameters pertaining to neutral amine molecules, parameters are evaluated for the ionized forms of the amines (i.e., for the methylammonium, morpholinium, N-methylmorpholinium, and N-ethylmorpholinium ions). For these ions, $\Delta\overline{G}_f^0$, $\overline{S}^0$ and the coefficients of the HKF equation are in most cases obtained by regressing the ionization equilibrium constants for the amines. In the case of morpholine, the ionization constants are used simultaneously with the apparent molar heat capacities and volumes of morpholine and morpholine chloride [33]. Thus, a complete set of HKF parameters can be evaluated for the morpholinium ion. For the remaining ions, only the $c_{HKF,i}$ coefficients of the HKF equation can be obtained on the basis of the temperature dependence of the amine ionization constant and the $a_{HKF,i}$ coefficients are set equal to zero.

In the second stage, parameters have been determined for amine hydrochlorides. For amine hydrochlorides, the experimental database includes solid–gas equilibria for pure salts, solid–liquid equilibria for binary mixtures of amine hydrochlorides with water and, in some cases, vapor–liquid equilibria for amine hydrochloride – water systems. Solid-gas equilibria depend on the thermochemical properties of the solid amine hydrochloride as well as on the gas-phase properties of the constituent amine and HCl (cf. Eqs. (8) and (9)). Accurate thermochemical properties of the solid phases are not available in the literature and need to be evaluated. In principle, the thermochemical properties of solid amine hydrochlorides could be determined from solid–gas equilibria considering that the relevant gas-phase properties are known from independent measurements (cf. Table 5) and that the heat capacity of the solid is either known from experimental measurements or can be estimated (cf. Table 6). However, the solid–gas equilibrium data are subject to substantial uncertainties which, in general, exceed the uncertainty of solid–liquid equilibria. Therefore, a better accuracy is obtained by simultaneously regressing the solid–gas equilibria for pure amine hydrochlorides and solid–liquid equilibria for binary mixtures of the hydrochlorides with water. The latter data are available over a substantial range of temperature, terminating at the melting point of pure amine hydrochlorides. In addition to the solid-phase thermochemical properties, the solid–liquid equilibria depend on the interactions between the amine-H^+ and Cl^- ions, which are reproduced using the ion-interaction term (Eqs. (20)–(23)). Thus, the thermochemical properties of the solid phase (i.e., $\Delta G_f^{S,0}$ and $S^{S,0}$) and the ion interaction parameters are obtained by simultaneously regressing solid–gas, solid–liquid and vapor–liquid equilibria for amine hydrochlorides and their mixtures with water. The ion-interaction parameters are listed in Table 2 and the solid-phase properties are collected in Table 6.

In the third step of model parameterization, parameters have been determined for amine – CO_2 – H_2O mixtures. Among the amines studied here, experimental data are available only for mixtures of morpholine with CO_2. For the morpholine – CO_2 – H_2O system, both vapor–liquid equilibrium and speciation data are available (cf. Table A-1). These data are regressed to obtain the

Table 1
Parameters for calculating the properties of individual solution species: standard partial molar Gibbs energy of formation, entropy, and parameters of the Helgeson–Kirkham–Flowers equation of state [24,37–39] for standard partial molar thermodynamic properties ($a_{HKF,1,\ldots4}$,$c_{HKF,1}$,$c_{HKF,2}$,ω).

Species	$\Delta\overline{G}_f^0$ J·mol^{-1}	$\overline{S}^0$ J·mol^{-1}K^{-1}	$a_{HKF,1}$	$a_{HKF,2}$	$a_{HKF,3}$	$a_{HKF,4}$	$c_{HKF,1}$	$c_{HKF,2}$	ω
Cl^{-} [a]	−131290	56.735	0.4032	480.1	5.563	−28470	−4.4	−57140	145600
H_3O^{+} [b]	−237175	69.994	0.451232	−21.2711	−8.64735	20487	14.6773	16976	−13672.5
$CH_3NH_{2(aq)}$ [c]	20131.69	138.7346	0	0	0	0	0	0	0
$CH_3NH_3^{+}$ [c]	−40431.83	156.4204	0	0	0	0	17.92915	64400.42	−6402.867
$O(CH_2CH_2)_2NH_{(aq)}$ [c]	1885.661	58.19216	0	0	0	0	0	0	0
$O(CH_2CH_2)_2NH_2^{+}$ [c]	−46574.99	89.33509	−18.20311	52052.25	0.654319	0	61.20571	−94975.94	−89643.28
$O(CH_2CH_2)_2NCH_{3(aq)}$ [c]	41026.26	89.41041	0	0	0	0	0	0	0
$O(CH_2CH_2)_2NHCH_3^{+}$ [c]	−1460.643	143.0357	2.279799	0	0	0	71.23958	0	0
$O(CH_2CH_2)_2NC_2H_{5(aq)}$ [c]	8998.403	240.6633	0	0	0	0	0	0	0
$O(CH_2CH_2)_2NHC_2H_5^{+}$ [c]	−35073.73	480.4759	0	0	0	0	0	0	0
$O(CH_2CH_2)_2NCOO^{-}$ [c]	−348555.9	39.61279	2.738048	0	−29.06707	0	30.77838	−37592.26	82390.7
$CO_{2(aq)}$ [b]	−385.974	117.57	1.50979	0.	−109.419	0.	40.0325	88004	−2000
HCO_3^{-} [a]	−586.940	98.4495	0.75621	115.05	1.2346	−28266	12.9395	−47579	127330
CO_3^{2-} [a]	−527983	−49.9988	0.28524	−398.44	6.4142	−26143	−3.3206	−171917	339140

[a] Parameters obtained from Shock and Helgeson [25], Shock et al. [26], and Johnson et al. [27].
[b] Parameters obtained in previous studies [18,19].
[c] Parameters determined in this study.

Table 2
Binary parameters used in the virial interaction term (Eqs. (22)–(23)).

Species i	Species j	$b_{0,ij}$	$b_{1,ij}$	$b_{2,ij}$	$c_{0,ij}$	$c_{1,ij}$	$c_{2,ij}$
$O(CH_2CH_2)_2NH$	H_2O	−2.259535	0	743.4495	0	0	0
$CH_3NH_3^+$	Cl^-	−12.15396	0.0236223	−128.6262	0	0	2450.963
$O(CH_2CH_2)_2NH_2^+$	Cl^-	29.17933	−0.06294247	624.4371	6.121036	0.09438822	−21673.98
$O(CH_2CH_2)_2NHCH_3^+$	Cl^-	−8.163352	0	−3976.503	0	0	11343.74
$O(CH_2CH_2)_2NHC_2H_5^+$	Cl^-	−17.40033	0	1198.504	0	0	6415.808
$O(CH_2CH_2)_2NCOO^-$	$O(CH_2CH_2)_2NH_2^+$	0	0	0	27.22975	0	−11830.99
$O(CH_2CH_2)_2NCOO^-$	$O(CH_2CH_2)_2NH$	0	0	0	27.22975	0	−11830.99
$O(CH_2CH_2)_2NCOO^-$	CO_2	0	0	0	−28.48946	0	13844.19
$O(CH_2CH_2)_2NH_2^+$	CO_2	0	0	0	48.15188	0	−16204.21
$O(CH_2CH_2)_2NH$	CO_2	0	0	0	48.15188	0	−16204.21
H_3O^+	Cl^-	75.511	−0.0858707	−21132.3	−167.683	0.228176	35827.5

Table 3
Binary parameters used in the short-range interaction term (Eq. (28)).

Species i	Species j	$a_{ij}^{(0)}$	$a_{ij}^{(1)}$	$a_{ij}^{(2)}$
CH_3NH_2	H_2O	−2612.727	1.866098	0
H_2O	CH_3NH_2	−5704.549	15.7434	0
$O(CH_2CH_2)_2NH$	H_2O	−219.5435	−21.05606	0.03819632
H_2O	$O(CH_2CH_2)_2NH$	−2484.09	38.19694	−0.07567502
$O(CH_2CH_2)_2NCH_3$	H_2O	31556.55	−72.31427	0
H_2O	$O(CH_2CH_2)_2NCH_3$	−6727.248	11.90043	0
$O(CH_2CH_2)_2NC_2H_5$	H_2O	20001.51	−39.87013	0
H_2O	$O(CH_2CH_2)_2NC_2H_5$	−4977.514	7.803552	0

Table 4
Liquid-phase heat capacity parameters and van der Waals volume and surface area.

Species	$C_p^L = a^L + b^L T + c^L T^2$, J/(mol·K)			References	r^c	q^c
	a^L	b^L	c^L			
CH_3NH_2[a]	92.520	0.03745	0	[40–42]	1.5959	1.544
$O(CH_2CH_2)_2NH$[a]	255.93	−0.63105	0.0011979	[43–45]	3.474	2.796
$O(CH_2CH_2)_2NCH_3$[b]	36.0	0.54915	0	[43]	3.474	2.796
$O(CH_2CH_2)_2NC_2H_5$[b]	45.5	0.54915	0	[43]	4.8024	3.880

[a] Parameters regressed to reproduce the experimental data as a function of temperature.
[b] Parameters obtained by assuming the same temperature dependence as for cyclohexylamine and matching a single experimental point.
[c] Obtained from Hansen et al. [46].

Table 5
Thermochemical properties of species in the gas phase.

Species	$\Delta G_f^{G,0}$ J·mol^{-1}	$S^{G,0}$ J·mol^{-1}K^{-1}	$C_p^G = a^G + b^G T + \frac{c^G}{T^2} + d^G T^2 + e^G T^3$					Ref.
			a^G	b^G	c^G	d^G	e^G	
CH_3NH_2	31761.9	242.9	15.9309	0.126881	0	−3.7248e-5	0	[40,47–51]
$O(CH_2CH_2)_2NH$	29700.69	232	−124.999	0.94766	2559960	−8.68689e-4	3.04031e-7	[43,52]
$O(CH_2CH_2)_2NCH_3$	56581.52	232	29.49932	0.285002	0.00364717	0	0	[43] [a]
$O(CH_2CH_2)_2NC_2H_5$	24855.43	382.585	0.8472	0.638249	0	−2.1322e-4	0	[43] [b]
HCl	−95300.0	186.901	30.0795	−0.006724	7858.39	1.2227e-5	−3.98114e-9	[40,53,54]
CO_2	−394.36	213.74	26.2022	0.051162	−169772	−2.9058e-5	6.20044e-9	[54,55]

[a] C_p based on that of morpholine, with a simplified temperature dependence.
[b] C_p based on that of ethylcyclohexane [40].

Table 6
Thermochemical properties of solid phases.

Species	$\Delta G_f^{S,0}$ J·mol^{-1}	$S^{S,0}$ J·mol^{-1}K^{-1}	$C_p^S = a^S + b^S T$	
			a^S	b^S
$CH_3NH_2 \cdot HCl$[a]	−158382	149.7764	55.3694	0.120072
$O(CH_2CH_2)_2NH \cdot HCl$[b]	−153222.6	256.6276	100	0
$O(CH_2CH_2)_2NC_2H_5 \cdot HCl$[b]	−160432	224.4664	100	0

[a] *Cp* obtained from Ashton and Zimmer [56]; $\Delta G_f^{S,0}$ and S^0 regressed in this study.
[b] *Cp* roughly estimated; $\Delta G_f^{S,0}$ and S^0 regressed in this study.

standard-state properties (i.e., $\Delta\overline{G}_f^0$ and $\overline{S}^0$) of the morpholine carbamate ion, $O(CH_2CH_2)_2NCOO^-$, and ion interaction parameters between the predominant species in the morpholine – CO_2–H_2O mixtures. Since no experimental data are available for a precise determination of the HKF coefficients of the carbamate ion, it has been assumed that the carbamate formation reaction (Eq. (3)) is accompanied by no change in the standard-state heat capacity and volume. This assumption makes it possible to estimate the HKF coefficients of the carbamate ion based on the properties of the other species that participate in reaction (3). The obtained standard-state parameters of the carbamate ion are given in Table 1 and the binary ion-interaction parameters are listed in Table 2. For completeness, Tables 1 and 2 also include the parameters for other species that are of interest here (e.g., Cl^-, H_3O^+, HCO_3^-, etc.) The parameters for such species were evaluated in previous studies as indicated in Tables 1 and 2.

3. Results and discussion

3.1. Amine – water systems

Figs. 2–7 compare the results obtained from the model with representative experimental data for amine – water binaries. For these binaries, vapor–liquid equilibria are the primary source of experimental information. The amines studied here strongly differ with respect to their volatility. Whereas methylamine is much more volatile than water, the morpholine derivatives are less volatile than water at moderate temperatures. Figs. 2 and 3 show vapor–liquid equilibrium projections for methylamine-water binary systems as a function of methylamine mole fraction and temperature, respectively. In the low methylamine concentration range shown in Fig. 2, the partial pressure of methylamine essentially follows Henry's law and depends primarily on the parameters $\Delta\overline{G}_f^0$ and $\overline{S}^0$. Although the experimental VLE data do not extend above the methylamine mole fraction of 0.486, the model can predict VLE in the complete range of concentrations because it is constrained to reproduce the vapor pressure of pure methylamine (cf. Table A-1). In the case of morpholine, experimental data in wide ranges of composition are available at moderate temperatures. The upper diagram in Fig. 4 shows the representation of the data at 75.2 and 95.2 °C. In common with most neutralizing amines, the morpholine – water system shows limited nonideality of the liquid phase.

When the amines are used in the power industry as volatile additives for pH control, the distribution coefficient of the amine is

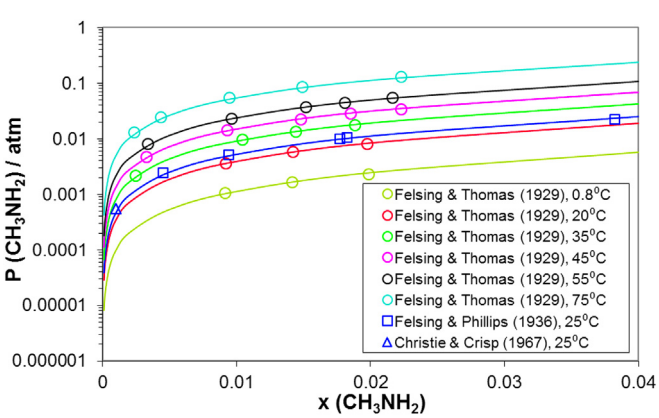

Fig. 2. Calculated and experimental partial pressure of methylamine in the methylamine – water mixture at temperatures ranging from 0.8 to 75 °C. The lines are obtained from the model and the experimental data are from Felsing and Thomas [59], Felsing and Phillips [63] and Christie and Crisp [64].

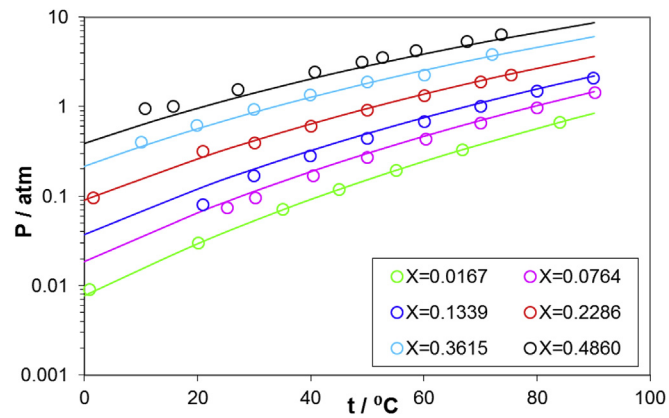

Fig. 3. Calculated and experimental total pressure in the system methylamine – water as a function of temperature for methylamine mole fractions ranging from 0.0167 to 0.486. The experimental data are from Bergstrom and Oloffson [60].

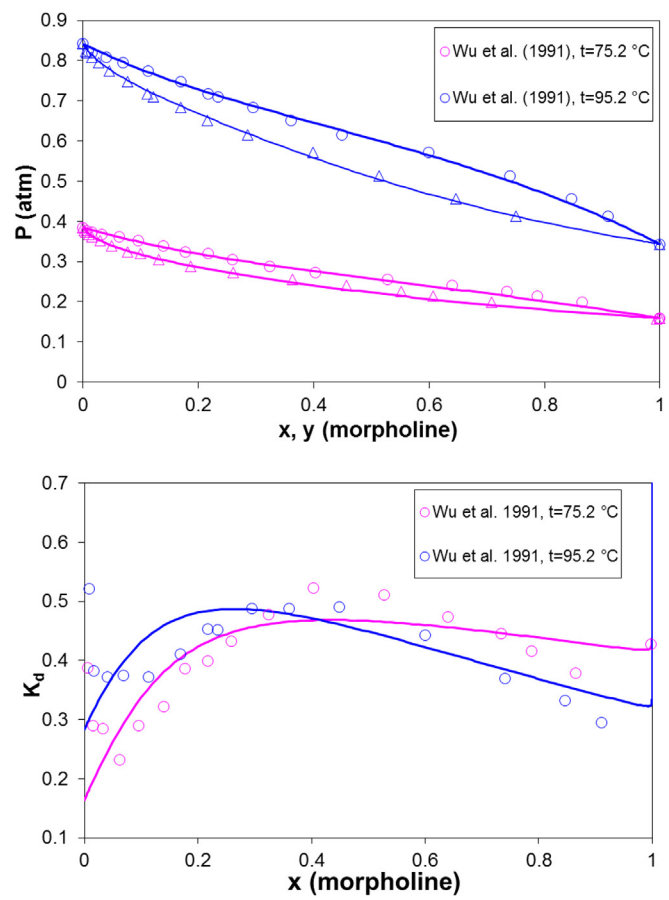

Fig. 4. Calculated and experimental [84] vapor–liquid equilibria in the system morpholine – water at 75.2 and 95.2 °C. The upper diagram is a classical P-x-y projection whereas the lower diagram shows the distribution coefficient of morpholine at the same conditions.

of particular interest. The distribution coefficient K_d, defined as the ratio of the concentration of the amine in the vapor phase to that in the liquid phase, provides a simple way to quantify the volatility of the amine. The knowledge of the volatility is important for assessing the ability of the amine to protect, via pH control, the areas exposed to wet steam and for evaluating the losses of the amine due to evaporation [8]. To illustrate the dependence of the

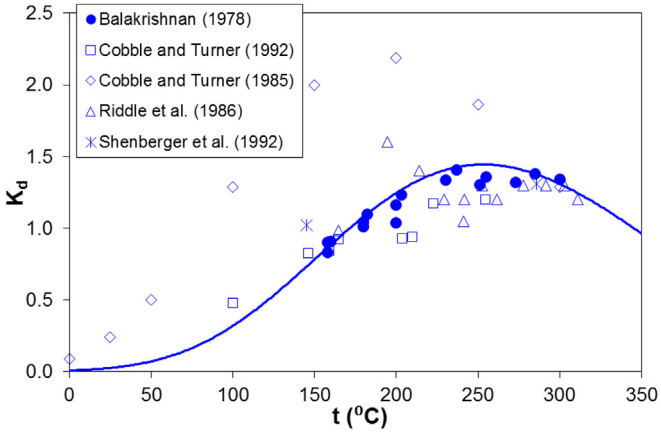

Fig. 5. Calculated and experimental distribution coefficient of morpholine in infinitely dilute aqueous solutions as a function of temperature along the water vapor–liquid saturation line. The experimental data are from Balakrishnan [8], Cobble and Turner [12,116], Riddle et al. [10], and Shenberger et al. [11].

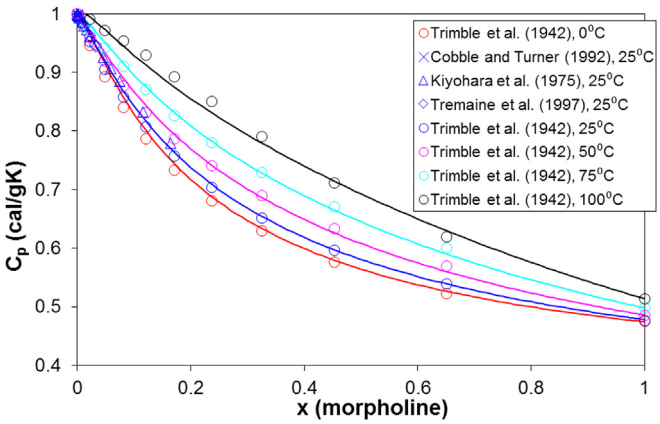

Fig. 6. Calculated and experimental heat capacity of binary morpholine – water mixtures at temperatures ranging from 0 to 100 °C. The experimental data are from Trimble et al. [44], Cobble and Turner [12], Kiyohara et al. [96], and Tremaine et al. [33].

distribution coefficient on morpholine concentration, the lower diagram in Fig. 4 restates the calculated results and experimental data in the form of K_d at the same conditions at which the "classical" P-x-y projection is shown in the upper diagram. In the low morpholine concentration range, which is of practical importance, K_d increases with morpholine concentration before reaching a maximum. Since the volatilities of morpholine and water are fairly similar, K_d remains in a relatively narrow range, i.e., approximately from 0.2 to 0.5. It is of interest that the computation of K_d amplifies the inherent uncertainty of experimental data in the low concentration range of the amine. This is shown by the large scattering of the data in the lower diagram of Fig. 4 at low morpholine concentrations whereas little scattering is observed in the P-x-y projection. This underscores the advantages of thermodynamic modeling based on a simultaneous analysis of various kinds of experimental data. By virtue of evaluating the model parameters from multi-property data in wide ranges of temperature and composition, a more reliable prediction of the distribution coefficient can be expected. This is particularly important at elevated temperatures, which are important in power generation.

Fig. 5 shows the calculated and experimental distribution coefficients of morpholine in dilute aqueous solutions at temperatures up to 350 °C. At 75.2 and 95.2 °C, the calculated K_d is

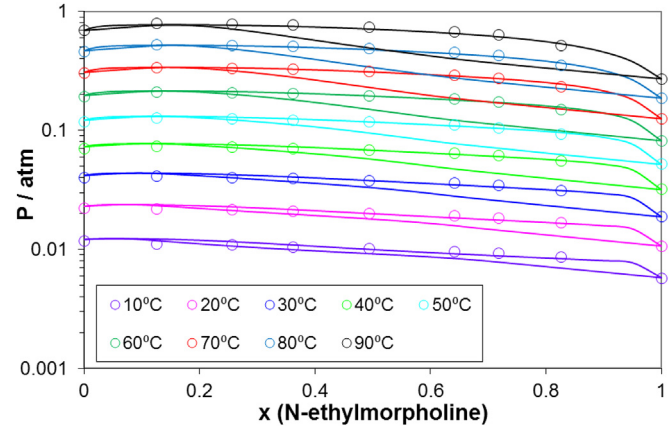

Fig. 7. Calculated and experimental vapor–liquid equilibria in the N-ethylmorpholine – water system at temperatures ranging from 10 to 90 °C. The experimental data are from Chiali-Baba-Ahmed et al. [111].

consistent with the infinite-dilution K_d values in Fig. 4. At higher temperatures, the infinite-dilution K_d substantially increases and exceeds 1 at approximately 170 °C before reaching a shallow maximum. While the experimental K_d data are fairly scattered, the model predictions agree well with the data of Balakrishnan [8]. Thus, the model is useful for differentiating between discordant data sets.

Experimental liquid-phase heat capacity data are particularly useful for constraining the temperature dependence of the model parameters. While pure-component liquid heat capacity data are available for all the amines studied here, heat capacity measurements in binary systems have been reported only for morpholine. As shown in Fig. 6, the model accurately reproduces the concentration and temperature dependence of the heat capacity of the morpholine – water binary system.

In the case of N-methylmorpholine and N-ethylmorpholine, experimental VLE data are available at temperatures up to ~100 °C. The VLE behavior of the mixtures of these two amines with water is fairly similar to that of the morpholine – water system. The calculated and experimental vapor–liquid equilibria for the N-ethylmorpholine – water mixture are shown in Fig. 7. While the volatility of pure N-ethylmorpholine is similar to that of

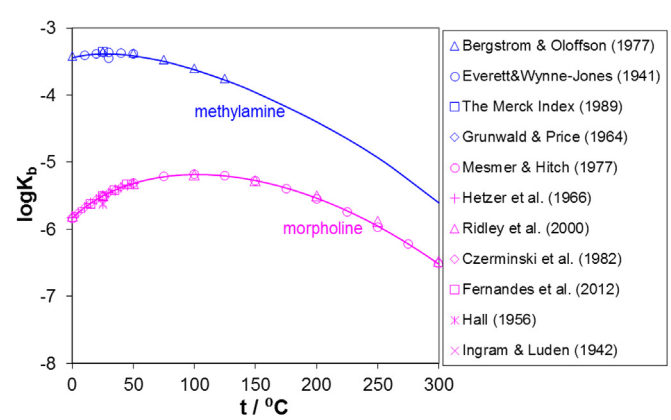

Fig. 8. Calculated and experimental dissociation constants for methylamine and morpholine. The experimental data for methylamine are from Bergstrom and Oloffson [60], Everett and Wynne–Jones [61], Merck Index [58], and Grunwald and Price [62] and those for morpholine are from Mesmer and Hitch [85], Hetzer et al. [86], Ridley et al. [87], Czerminski et al. [88], Fernandes et al. [89], Hall [90], and Ingram and Luden [92].

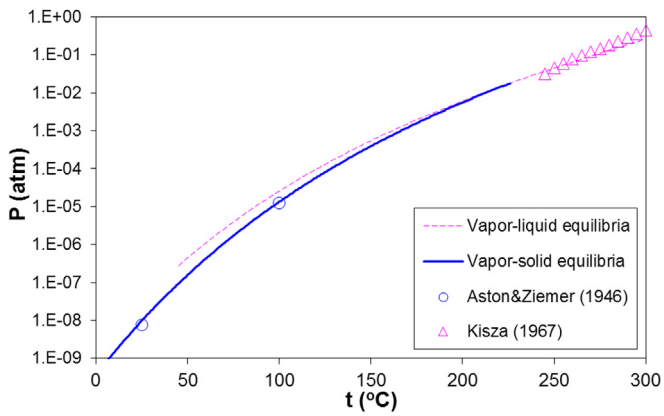

Fig. 9. Vapor–solid and vapor–liquid equilibria for pure methylamine hydrochloride. The solid line shows the vapor–solid equilibrium and the dashed line shows the vapor–liquid equilibrium, including a metastable extension below the triple point of methylamine hydrochloride. The experimental VLE and VSE data are from Kisza [65] and Aston and Ziemer [56], respectively.

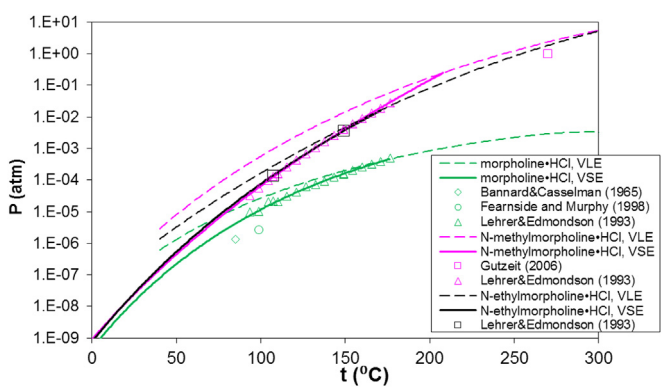

Fig. 10. Vapor pressures of solid (solid lines) and liquid (dashed lines) hydrochlorides of morpholine, N-methylmorpholine, and N-ethylmorpholine. The dashed lines are extended into the metastable region of liquid amine hydrochlorides below their triple points. The experimental data are from Lehrer and Edmondson [34] (for all three amine hydrochlorides), Bannard and Casselman [99] and Fearnside and Murphy [100] (for morpholine hydrochloride) and Gutzeit [4] (for N-methylmorpholine hydrochloride).

morpholine, the nonideality of the N-ethylmorpholine – water binary is larger due to the presence of an additional ethyl group and the absence of a hydrogen that can participate in hydrogen bonding. This manifests itself in an azeotrope with the azeotropic composition shifting with temperature towards higher amine mole fractions.

As indicated by reactions (1) and (2), amines undergo hydrolysis reactions and are weak bases. The equilibrium constants of reactions (1) and (2) have been investigated in a particularly wide temperature range (i.e., up to 300 °C) for morpholine because of its wide use in electrical power generation (cf. Table A-1). Fig. 8 shows the temperature dependence of the dissociation constants, K_b, for the amines for which experimental data are available in the widest temperature ranges, i.e., for methylamine and morpholine. It should be noted that the maximum in the dissociation constant is a common feature of most amines although the location of the maximum differs depending on the structure of the amine. The maximum is accurately represented by calculating the standard-state properties of the ammonium ions from the HKF equation and using them in conjunction with those for molecular amines.

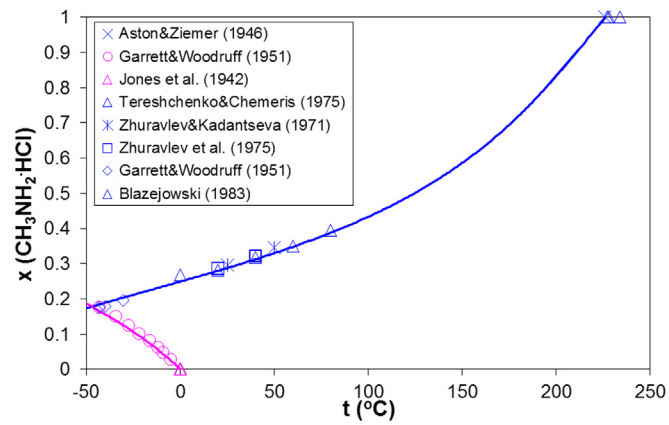

Fig. 11. Calculated and experimental solid–liquid equilibria in the system methylamine hydrochloride – water. The ice solubility data are from Garrett and Woodruff [70] and Jones et al. [71] and the methylamine hydrochloride solubility measurements are from Aston and Ziemer [56], Tereshchenko and Chemeris [67], Zhuravlev and Kadantseva [68], Zhuravlev et al. [69], Garrett and Woodruff [70], and Blazejowski [66].

3.2. Pure amine hydrochlorides

Unlike most pure components, amine hydrochlorides undergo a chemical reaction in conjunction with their sublimation or melting. This is due to the fact that amine hydrochlorides do not exist in a molecular form in the gas phase and decompose to the constituent amine and hydrogen chloride molecules. The sublimation reaction for the amine hydrochlorides considered here is given by Eqs. (8) and (9). In the case of melting, Eqs. (10) and (11) describe the reactions that accompany both the melting of pure amine hydrochlorides and the solid–liquid equilibrium in amine hydrochloride-water solutions. Fig. 9 shows the equilibrium pressure for the reactive vapor–solid and vapor–liquid equilibria of pure methylamine hydrochloride as a function of temperature. The solid line indicates vapor–solid equilibrium whereas the dashed line depicts vapor–liquid equilibrium. The two lines intersect at 226 °C at the triple point of the amine hydrochloride, which is very close to the experimentally measured melting point. The dashed vapor–liquid line is extended towards lower temperatures (i.e., within the metastable range of the liquid) to indicate the change in the slope of the two equilibrium curves at the triple point. The model accurately represents the available experimental data for both vapor–solid and vapor–liquid equilibria. The low equilibrium pressures in the

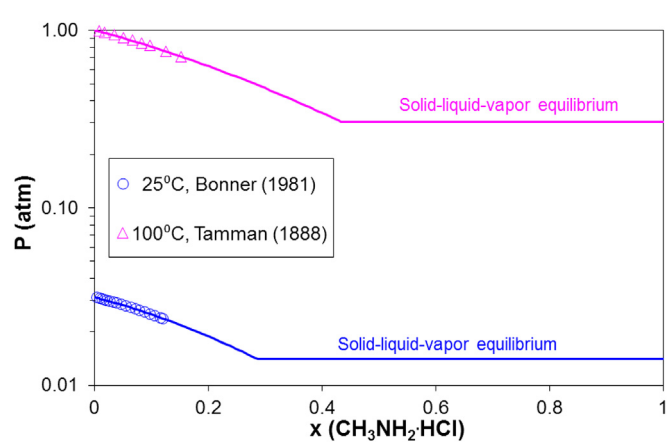

Fig. 12. Calculated and experimental vapor–liquid equilibria in the system methylamine hydrochloride – water at 25 and 100 °C. The experimental data are from Bonner [73] and Tamman [72].

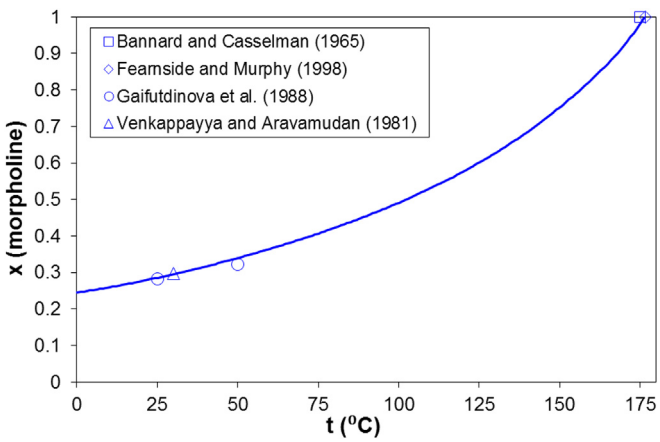

Fig. 13. Calculated and experimental solid liquid equilibria for morpholine – water mixtures. The experimental data are from Bannard and Casselman [99], Fearnside [100], Gaifutdinova et al. [101] and Venkappaya and Aravamudan [102].

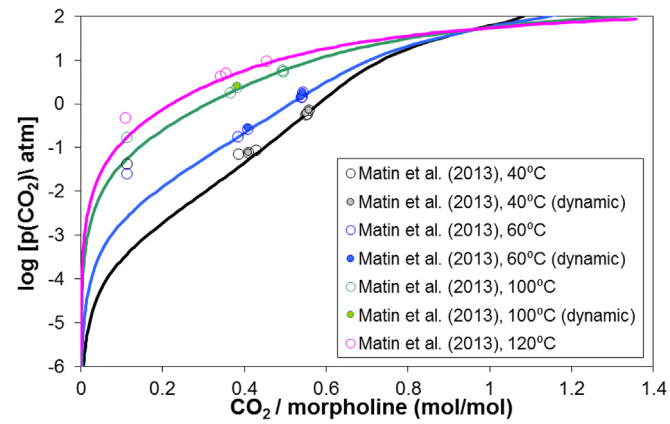

Fig. 14. Calculated and experimental partial pressure of CO_2 as a function of CO_2 loading in the system morpholine – CO_2 – H_2O with the morpholine molality of 8.84. The experimental data are from Matin et al. [98].

temperature range below ca. 140 °C are particularly important because they are associated with the strong driving force for the formation of the solid hydrochloride in refinery overhead environments even when the partial pressures of methylamine and HCl in the gas phase are fairly low.

Fig. 10 compares the vapor–solid and vapor–liquid equilibria for the hydrochlorides of morpholine and its N-methyl and N-ethyl derivatives. For these salts, experimental data are available primarily for solid–gas equilibria. It has been observed that the vapor pressures of Lehrer and Edmondson [34], which are available for ammonium chloride as well as for the amine hydrochlorides, are somewhat lower for ammonium chloride than the generally accepted data [35,36]. Therefore, a correction factor has been obtained at each temperature by calculating a ratio of Lehrer and Edmondson's [34] NH_4Cl equilibrium pressures to those of Stull [35] and Braden et al. [36] and, subsequently, applying this correction to Lehrer and Edmondson's [34] amine hydrochloride data. In this way, a set of data has been obtained that are consistent with other data for the hydrochlorides of morpholine derivatives, including solid–liquid equilibrium and melting point data. As illustrated in Fig. 10, the equilibrium pressures of N-methyl- and N-ethylmorpholine are very close to each other and are appreciably higher than those of unsubstituted morpholine. This can be attributed to the lack of hydrogen bonding in N-methyl- and N-ethylmorpholine, which can be expected to increase volatility. Thus, unsubstituted morpholine is more prone to form a solid hydrochloride salt in refinery environments than its alkyl derivatives.

3.3. Amine hydrochloride – water mixtures

In general, solid–liquid and vapor–liquid equilibria in the amine hydrochloride – water mixtures provide somewhat more precise information about the thermodynamic properties of amine hydrochlorides than the solid–gas equilibrium pressure measurements. Fig. 11 shows the solid–liquid equilibria in the methylamine hydrochloride – water system. The SLE curve in Fig. 11 has two branches. The lower branch represents the solubility of ice whereas the upper branch is the solubility of solid methylamine hydrochloride. The upper branch terminates at the melting point of pure methylamine hydrochloride (226 °C). The two branches intersect at the eutectic temperature at −46 °C. For this system, experimental data from various sources are in a good agreement. VLE data are available for methylamine hydrochloride solutions only at relatively low methylamine hydrochloride mole fractions, i.e., up to ca. 0.15. Fig. 12 compares the calculated and experimental VLE results in this system for two isotherms (25 °C and 100 °C). The horizontal portion of the VLE curve starts at the solubility point at each temperature (consistent with Fig. 11) and corresponds to three-phase solid–liquid–vapor equilibria, for which the equilibrium pressure is constant. The model represents both the SLE and VLE data in the complete concentration and temperature ranges within experimental uncertainty.

In the case of the morpholine hydrochloride – water system, the available SLE data are less extensive and are limited to one branch, i.e., the solubility of morpholine hydrochloride. The calculated SLE curve is shown in Fig. 13 and bears a strong similarity to that for methylamine hydrochloride. For N-methyl- and N-ethylmorpholine, the experimental SLE data are limited to the melting points of pure amine hydrochlorides. Nevertheless, SLE can be predicted for these amines using the solid-phase thermodynamic properties obtained from solid–gas equilibrium data (cf. Fig. 10).

In general, a characteristic feature of SLE in amine hydrochloride – water systems is the lack of hydrated solid phases. Such hydrated phases have not been identified for amine hydrochlorides even though they are very common for the majority of inorganic salts. Therefore, the solubility curves of amine hydrochlorides have a common shape, extending uninterruptedly from the eutectic point

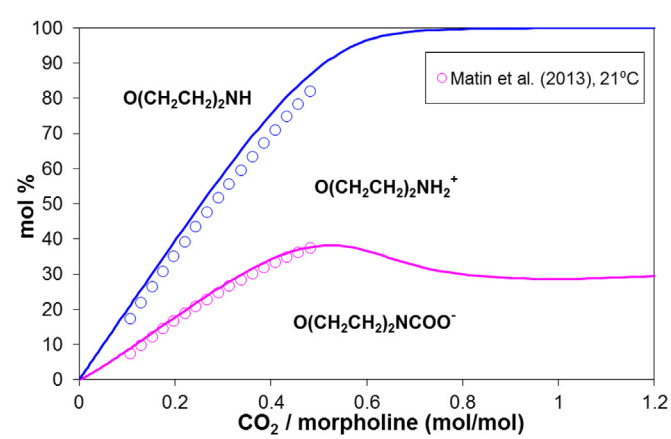

Fig. 15. Speciation in the system morpholine – CO_2 – H_2O with the morpholine molality of 8.84. The areas delimited by the lines denote the relative amounts of neutral morpholine, $O(CH_2CH_2)NH$, morpholinium ion, $O(CH_2CH_2)NH_2^+$, and morpholine carbamate ion, $O(CH_2CH_2)NCOO^-$. The experimental data are from Matin et al. [98].

with ice at low temperatures up to the melting point of a pure amine hydrochloride. As a corollary, the solubility of amine hydrochlorides can be predicted from solid–gas data for pure hydrochlorides because the solubility behavior is not complicated by hydrates.

3.4. Amine – water – CO_2 systems

Carbon dioxide is ubiquitous in refinery applications and, despite being a much weaker acid than HCl, may affect the formation of amine hydrochlorides by contributing to the neutralization of amines and by forming carbamate ions. CO_2 is also present in power generation environments (e.g. from in-leakage of air or from the decomposition of carbonates), in which it is the main source of acidity. Thus, the effects of HCl and CO_2 need to be considered simultaneously in the simulation of the performance of neutralizing amines. Among the amines that are considered here, data in the presence of CO_2 are available only for morpholine. Fig. 14 compares the calculated and experimental partial pressures of CO_2 as a function of the CO_2 loading (i.e., the CO_2/morpholine molar ratio) at temperatures up to 120 °C. A corresponding speciation plot is shown in Fig. 15, in which the relative amounts of the species are indicated by the areas delimited by the lines. The model simultaneously reproduces the VLE and speciation data. As shown in Fig. 15, the fraction of neutral amine, $O(CH_2CH_2)_2NH$, rapidly diminishes with increasing CO_2/morpholine ratio and becomes negligible as the ratio exceeds ca. 0.6. The fractions of the morpholinium ion, $O(CH_2CH_2)_2NH_2^+$, and the morpholine carbamate ion, $O(CH_2CH_2)_2NCOO^-$, increase with the CO_2/morpholine ratio and reach fairly constant values at the ratios above ca. 0.7. Thus, the significant concentration of the carbamate ion can be expected to interfere with the formation of amine hydrochloride salts.

3.5. Model applications

As described by Patel et al. [5] and Armistead et al. [6], the combined model can be applied to predict the behavior of neutralizing amines in refinery overhead environments. Specifically, it has been used to study the evolution of the phase behavior of refinery streams as a function of temperature. Although a detailed analysis of such applications is beyond the scope of this study, it is worth noting that the corrosive properties of streams can be analyzed by calculating three characteristic quantities, i.e., the salt point, ionic dew point, and water dew point [6]. The salt point is the temperature at which a solid amine hydrochloride precipitates from the gas phase and indicates the possibility of solid phase deposition downstream. The ionic dew point is the temperature that corresponds to the incipient formation of a typically small amount of a concentrated aqueous amine hydrochloride solution, which is highly corrosive. Finally, the water dew point is the temperature (or temperature range) at which the bulk of the water in the stream starts to condense, forming a dilute and typically non-corrosive aqueous solution. In general, it is desirable to minimize the temperature range between the ionic dew point and water dew point because the corrosive amine hydrochloride solution exists in this range. This can be achieved by modifying the stream conditions, implementing water washing, and optimizing the selection of amines. As discussed by Armistead et al. [6], the model can be used as a computational tool for this purpose.

4. Conclusions

A comprehensive modeling framework has been developed for calculating phase and chemical equilibria in systems containing amines, amine hydrochlorides, water, HCl, and CO_2. For this purpose, the previously developed Mixed-Solvent Electrolyte (MSE) model has been extended to represent simultaneously solid–gas, solid–liquid, and vapor–liquid equilibria, speciation, and liquid-phase caloric properties. This framework is particularly suitable for systems that range from weak electrolytes (i.e., amine – water mixtures) to strong electrolytes (i.e., amine hydrochloride – water mixtures from pure water to pure molten amine hydrochloride). The model has been parameterized for systems containing methylamine, morpholine, N-methylmorpholine, N-ethylmorpholine and their corresponding hydrochlorides. It can be used as a computational tool for simulating phase behavior in refinery environments and, in particular, for predicting the corrosivity of streams that is caused by the formation of concentrated amine hydrochloride solutions.

Acknowledgment

This work was supported by Athlon, Baker Hughes, BP, Chevron, ConocoPhillips, ExxonMobil, Honeywell, Nalco, Petrobras, Saudi Aramco, Shell, Sunoco, and Total.

Appendix

Table A-1
Sources of experimental data for aqueous systems containing methylamine, morpholine, N-methylmorpholine, N-ethylmorpholine and their hydrochlorides.

System	Data type	Temperature range, K	References
Methylamine	Vapor pressure	177–267	Stull [35]
		190–267	Timmermans [57]
		199–283	TRC [40]
		199–267	Merck Index [58]
		190–267	Aston et al. [41]
		193–430	Felsing and Thomas [59]
	Liquid heat capacity	187–259	Aston et al. [41]
		188–260	Aston and Eidinoff [42]
		180–300	TRC [40]
	Gas heat capacity	298–1000	Rihani [47]
		298	Wagman et al. [48]
		298–1000	Stull et al. [49]
		298–1000	Seha [50]
		200–1400	Draeger et al. [51]
		50–1500	TRC [40]
Methylamine-H_2O	Dissociation equilibria	273–398	Bergström and Oloffsen [60]
		283–323	Everett and Wynner-Jones [61]
		298	Merck Index [58]

Table A-1 (*continued*)

System	Data type	Temperature range, K	References
		298	Grunwald and Price [62]
	Vapor – liquid equilibria	274–353	Felsing and Thomas [59]
		298	Felsing and Phillips [63]
		298	Christie and Crisp [64]
Methylamine hydrochloride	Solid – vapor pressure	298–373	Aston and Ziemer [56]
	Liquid – vapor pressure	518–573	Kisza [65]
	Heat capacity	266–298	Aston and Ziemer [56]
Methylamine hydrochloride-H_2O	Solid–liquid equilibria	499	Aston and Ziemer [56]
		501–507	Błażejowski [66]
		273–353	Tereshchenko and Chemeris [67]
		298–323	Zhuravlev and Kadantseva [68]
		293–313	Zhuravlev et al. [69]
		230–268	Garrett and Woodruff [70]
		273	Jones et al. [71]
		373	Tamman [72]
		298	Bonner [73]
		298	Macaskill and Penthybridge [74]
Morpholine	Vapor pressure	283–398	Bolling et al. [75]
		318–402	Palczewska-Tulińska et al. [76]
		293, 402	Merck Index [58]
		274–304	Verevkin [43]
		293–402	Savescu et al. [77]
		273–318	Cabani et al. [78]
		373–393	Lee et al. [79]
		356–401	Marrufo et al. [80]
		364–391	Pettenati et al. [81]
		402	Simoiu and Iacob [82]
		286, 401	Wilson [83]
		346–402	Wu et al. [84]
	Liquid heat capacity	273––403	Trimble et al. [44]
		298–353	Lyashkov [45]
		298	Verevkin [43]
	Gas heat capacity	100–500	Vedal et al. [52]
Morpholine-H_2O	Dissociation equilibria	273–573	Mesmer and Hitch [85]
		273–323	Hetzer et al. [86]
		273–573	Ridley et al. [87]
		278–313	Czerminski et al. [88]
		288–338	Fernandes et al. [89]
		298	Hall [90]
		273–323	Vistad et al. [91]
		298	Ingram and Luder [92]
	Vapor – liquid equilibria	348–368	Wu et al. [84]
		375–398	Savescu et al. [77]
		373–396	Skorokhodova et al. [93]
		355–387	Sovova and Boublik [94]
		373–401	Palczewska-Tulinska et al. [76]
		373–399	Wilson [83]
		431–573	Balakrishnan [8]
		555	Feron and Lambert [95]
		438–584	Riddle et al. [10]
		418, 559	Shenberger et al. [11]
		373–528	Cobble and Turner [12]
	Heat capacity	273–403	Trimble et al. [44]
		283–328	Tremaine et al. [33]
		298	Kiyohara et al. [96]
		298	Cobble and Turner [12]
Morpholine-CO_2-H_2O	Vapor – liquid equilibria	298–333	Al-Juaied and Rochelle [97]
		294–393	Matin et al. [98]
	Speciation	294	Matin et al. [98]
Morpholine hydrochloride	Solid – vapor pressure	358	Bannard and Casselman [99]
		372	Fearnside and Murphy [100]
		366–422	Lehrer and Edmondson [34]
Morpholine hydrochloride-H_2O	Solid–liquid equilibria	448	Bannard and Casselman [99]
		450	Fearnside and Murphy [100]
		298, 323	Gaifutdinova et al. [101]
		303	Venkappayya and Aravamudan [102]
N-methylmorpholine	Vapor pressure	276–319	Cabani et al. [78]
		293, 388	Wilson [83]
		293, 389	Huntsman [103]
		273–303	Verevkin [43]
		313–363	Belabbaci et al. [104]
		323–379	Fele et al. [105]
		389	Merck Index [58]
	Liquid heat capacity	298	Verevkin [43]

(*continued on next page*)

Table A-1 (*continued*)

System	Data type	Temperature range, K	References
N-methylmorpholine-H_2O	Dissociation equilibria	298	Hall [106]
		288–333	Xu et al. [107]
		293	Huntsman [103]
		298	Cabani et al. [108]
		298	Blais et al. [109]
	Vapor – liquid equilibria	313–363	Belabbaci et al. [104]
		334–370	Fele et al. [105]
N-methylmorpholine hydrochloride	Solid – vapor pressure	366–450	Lehrer and Edmondson [34]
	Liquid – vapor pressure	543	Gutzeit [4]
N-methylmorpholine hydrochloride-H_2O	Solid–liquid equilibria	477	Gutzeit [4]
		478	Knorr [110]
N-ethylmorpholine	Vapor pressure	274–313	Verevkin [43]
		273–363	Chiali-Baba-Ahmed et al. [111]
		293, 411	Huntsman [112]
	Liquid heat capacity	298	Verevkin [43]
N-ethylmorpholine-H_2O	Dissociation equilibria	298	Hall [106]
		298	Blais et al. [109]
		293	Huntsman [112]
		298	Goldberg et al. [113]
		298–318	Anwar and Sung [114]
	Vapor – liquid equilibria	283–363	Chiali-Baba-Ahmed et al. [111]
		~373	Ovejero et al. [115]
N-ethylmorpholine hydrochloride	Solid – vapor pressure	380–422	Lehrer and Edmondson [34]

References

[1] D.P. Valenzuela, A.K. Dewan, Refinery crude column overhead corrosion control, amine neutralizer electrolyte thermodynamics, thermochemical properties and phase equilibria, Fluid Phase Equilib. 158–160 (1999) 829–834.
[2] V.K. Braden, P.R. Petersen, Crude Unit Overhead Corrosion Control, CORROSION 1998, paper no. 585, NACE International, 1998.
[3] R. Rechtien, G.G. Duggan, Identifying the Impacts of Amine Contamination on Crude Units, CORROSION 2006, paper no. 06581, NACE International, 2006.
[4] J. Gutzeit, Crude Unit Corrosion Guide. A Complete How-to Manual, PCC, 2006.
[5] A. Patel, E. Vetters, A. Anderko, M. Lencka, Use of Ionic Modeling to Gain New Insights on Crude Unit Overhead Corrosion, CORROSION 2012, paper no. C2012–0001209, NACE International, 2012.
[6] K. Armistead, D. Leslie, R. Strong, Crude Unit Overhead Corrosion Control Successfully Driven by Ionic Modeling, CORROSION/2015, paper no. 6010, NACE International, 2015.
[7] D.D. Macdonald, G.A. Cragnolino, Corrosion of steam cycle materials, in: P. Cohen (Ed.), The ASME Handbook on Water Technology for Thermal Power Systems, American Society of Mechanical Engineers, New York, NY, 1989.
[8] P.V. Balakrishnan, Volatility of amines used for water treatment in steam generating systems, Can. J. Chem. 56 (1978) 2620–2623.
[9] D. Wesolowski, P. Bénézeth, D. Palmer, L. Anovitz, Protonation Constants of Morpholine, Dimethylamine and Ethanolamine to 290 °C and the Effect of Morpholine and Dimethylamine on the Surface Charge of Magnetite at 150–250 °C, EPRI Report 1003179, EPRI, Palo Alto, CA, 2002.
[10] J.M. Riddle, G.D. Burns, L.J. Cain, Chemistry Control With Morpholine at Beaver Valley Power Station, Report NP-4623, Electric Power Research Institute, Palo Alto, CA, 1986.
[11] D.M. Shenberger, J.D. Zupanovich, J.L. Walker, N.W. Nolan, Loop Testing of Alternative Amines for All-volatile Treatment Control in PWRs, Report TR-100756, EPRI, Palo Alto, CA, 1992.
[12] J.W. Cobble, P.J. Turner, PWR Advanced All-volatile Treatment Additives, By-products, and Boric Acid, Report TR-100755, Electric Power Research Institute, Palo Alto, CA, 1992.
[13] P. Wang, A. Anderko, R.D. Young, A speciation-based model for mixed-solvent electrolyte systems, Fluid Phase Equilib. 203 (2002) 141–176.
[14] P. Wang, R.D. Springer, A. Anderko, R.D. Young, Modeling phase equilibria and speciation in mixed-solvent electrolyte systems, Fluid Phase Equilib. 222 (2004) 11–17.
[15] P. Wang, A. Anderko, R.D. Springer, R.D. Young, Modeling phase equilibria and speciation in mixed-solvent electrolyte systems: II. Liquid-liquid equilibria and properties of associating electrolyte solutions, J. Mol. Liq. 125 (2006) 37–44.
[16] J.J. Kosinski, P.M. Wang, R.D. Springer, A. Anderko, Modeling acid-base equilibria and phase behavior in mixed-solvent electrolyte systems, Fluid Phase Equilib. 256 (2007) 34–41.
[17] P. Wang, J.J. Kosinski, A. Anderko, R.D. Springer, M.M. Lencka, J. Liu, Ethylene glycol and its mixtures with water and electrolytes: thermodynamic and transport properties, Ind. Eng. Chem. Res. 52 (2013) 15968–15987.
[18] R.D. Springer, Z. Wang, A. Anderko, P. Wang, A.R. Felmy, A thermodynamic model for predicting mineral reactivity in supercritical carbon dioxide: I. Phase behavior of carbon dioxide – water – chloride salt systems across the H_2O-rich to the CO_2-rich regions, Chem. Geol. 322–323 (2012) 151–171.
[19] R.D. Springer, P. Wang, A. Anderko, Modeling the properties of H_2S – CO_2 – salt – water systems in wide ranges of temperature and pressure, SPE J. 20 (2015) 1120–1134.
[20] M.S. Gruszkiewicz, D.A. Palmer, R.D. Springer, P.M. Wang, A. Anderko, Phase behavior of aqueous Na-K-Mg-Ca-Cl-NO_3 mixtures: isopiestic measurements and thermodynamic modeling, J. Solut. Chem. 36 (2007) 723–765.
[21] P. Wang, A. Anderko, Modeling chemical equilibria, phase behavior, and transport properties in ionic liquid systems, Fluid Phase Equilib. 302 (2011) 74–82.
[22] J.F. Zemaitis Jr., D.M. Clark, M. Rafal, N.C. Scrivner, Handbook of Aqueous Electrolyte Thermodynamics, American Institute of Chemical Engineers, New York, NY, 1986.
[23] M. Rafal, J.W. Berthold, N.C. Scrivner, S.L. Grise, Models for Electrolyte Solutions, in: S.I. Sandler (Ed.), Models for Thermodynamic and Phase Equilibria Calculations, Marcel Dekker, New York, NY, 1995.
[24] J.C. Tanger, H.C. Helgeson, Calculation of the thermodynamic and transport properties of aqueous species at high pressures and temperatures: revised equations of state for the standard partial molal properties of ions and electrolytes, Am. J. Sci. 288 (1988) 19–98.
[25] E.L. Shock, H.C. Helgeson, Calculation of the thermodynamic and transport properties of aqueous species at high pressures and temperatures: correlation algorithms for ionic species and equation of state predictions to 5 kb and 1000°C. Geochim. Cosmochim. Acta 52 (1988) 2009–2036.
[26] E.L. Shock, H.C. Helgeson, D.A. Sverjensky, Calculation of the thermodynamic and transport properties of species at high pressures and temperatures: standard partial molar properties of inorganic neutral species, Geochim. Cosmochim. Acta 53 (1989) 2157–2183.
[27] J.W. Johnson, E.H. Oelkers, H.C. Helgeson, SUPCRT92-A software package for calculating the standard molal thermodynamic properties of minerals, gases, aqueous species, and reactions from 1 bar to 5000 bar and 0 °C to 1000 °C, Comput. Geosci. 18 (1992) 899–947.
[28] L. Haar, J.S. Gallagher, G.S. Kell, NBS/NRC Steam Tables: Thermodynamic and Transport Properties and Computer Programs for Vapor and Liquid States in SI Units, Hemisphere Publishing, Washington, DC, 1984.
[29] K.S. Pitzer, Electrolytes – from dilute solutions to fused salts, J. Am. Chem. Soc. 102 (1980) 2902–2906.
[30] D.S. Abrams, J.M. Prausnitz, Statistical thermodynamics of liquid mixtures – new expressions for excess Gibbs energy of partly or completely miscible systems, AIChE J. 21 (1975) 116–128.
[31] K.S. Pitzer, Thermodynamics, third ed., McGraw-Hill, New York, 1995.
[32] G. Soave, Equilibrium constants from a modified Redlich–Kwong equation of state, Chem. Eng. Sci. 27 (1972) 1197–1203.
[33] P.R. Tremaine, D. Shvedov, C. Xiao, Thermodynamic properties of aqueous morpholine and morpholinium chloride at temperatures from 10 to 300 C: apparent molar volumes, heat capacities, and temperature dependence of ionization, J. Phys. Chem. B 101 (1997) 409–419.
[34] S.E. Lehrer, J.G. Edmondson, Neutralizing amines with low salt precipitation potential, United States Patent 5211840, 1993.
[35] D.R. Stull, Vapor pressure of pure substances, Ind. Eng. Chem. 39 (1947) 517–540.
[36] V.K. Braden, P. Fearnside, C.J. Murphy, Amine blend neutralizers for refinery process corrosion, United States Patent 5965785, (1999).

[37] H.C. Helgeson, D.H. Kirkham, G.C. Flowers, Theoretical prediction of the thermodynamic behavior of aqueous electrolytes at high pressures and temperatures. I Summary of the thermodynamic/electrostatic properties of the solvent, Am. J. Sci. 274 (1974) 1089–1198.
[38] H.C. Helgeson, D.H. Kirkham, G.C. Flowers, Theoretical prediction of the thermodynamic behavior of aqueous electrolytes at high pressures and temperatures. III Equation of state for aqueous species at infinite dilution, Am. J. Sci. 276 (1976) 97–240.
[39] H.C. Helgeson, D.H. Kirkham, G.C. Flowers, Theoretical prediction of the thermodynamic behavior of aqueous electrolytes at high pressures and temperatures. IV. Calculation of activity coefficients, osmotic coefficients, and apparent molal and standard and relative partial molal properties to 5 kb and 600°C, Am. J. Sci. 281 (1981) 1241–1516.
[40] Thermodynamics Research Center, Selected Values of Properties of Chemical Compounds Data Project, Texas A&M University, College Station, TX, 1980-1991.
[41] J.G. Aston, C.W. Siller, G.H. Messerly, Heat capacities and entropies of organic compounds. III. Methylamine from 11.5 K to the boiling point. Heat of vaporization and vapor pressure. The entropy from molecular data, J. Am. Chem. Soc. 59 (1937) 1743–1751.
[42] J.G. Aston, M.L. Eidinoff, The low temperature precision adiabatic calorimeter adapted to condensed gases from 10 K to room temperature, J. Am. Chem. Soc. 61 (1939) 1533–1538.
[43] S.P. Verevkin, Thermochemistry of amines: strain in six-membered rings from experimental standard molar enthalpies of formation of morpholines and piperazines, J. Chem. Thermodyn. 30 (1998) 1069–1079.
[44] H.M. Trimble, C.J. Engle, R.A. Brown, R.F. Schmuck, The specific heats of morpholine and its aqueous solutions, J. Am. Chem. Soc. 64 (1942) 679–681.
[45] V.I. Lyashkov, Thermal characteristics of morpholine, Izv. Vyssh. Uchebn. Zaved. Khim. Khim. Tekhnol. 23 (1980) 1085–1086.
[46] H.K. Hansen, P. Rasmussen, A. Fredenslund, Vapor-liquid equilibria by UNIFAC group contribution. 5. Revision and extension, Ind. Eng. Chem. Res. 30 (1991) 2355–2358.
[47] D.N. Rihani, Thermodynamic data for n-aminoalkanes, Hydrocarb. Process 47 (1968) 111–119.
[48] D.D. Wagman, W.H. Evans, V.B. Parker, I. Halow, S.M. Bailey, R.H. Schumm, Selected Values of Chemical Thermodynamic Properties, NBS Technical Note, 270-3, 1968.
[49] D.R. Stull, E.F. Westrum Jr., G.C. Sinke, The Chemical Thermodynamics of Organic Compounds, John Wiley & Sons, New York, NY, 1969.
[50] Z. Seha, Thermodynamische Funktionen Organischer Verbindungen III. Funktionen der Methylamine und des Formamides, Coll. Czech. Chem. Commun. 26 (1961) 2435–2438.
[51] J.A. Draeger, R.H. Harrison, W.D. Good, Chemical thermodynamic properties of molecules that undergo inversion. Aniline, methylamine, cyclopropylamine and cyclopentene, J. Chem. Thermodyn. 15 (1983) 367–376.
[52] D. Vedal, O.H. Ellestad, P. Klaboe, The vibrational spectra of piperidine and morpholine and their N-deuterated analogs, Spectrochim. Acta 32A (1976) 877–890.
[53] V.P. Glushko, V.A. Medvedev, G.A. Bergman, L.V. Gurvich, V.S. Yungman, A.F. Vorob'ev, V.P. Kolesov, L.A. Reznitskii, V.V. Mikhailov, G.L. Gal'chenko, M.K. Karapet'yans, Thermal Constants of Compounds, vols. I–III, Academy of Sciences of USSR, Moscow, 1965–1968.
[54] L.V. Gurvich, I.V. Veyts, C.B. Alcock, Thermodynamic Properties of Individual Substances, fourth ed., Hemisphere Publishing Corporation, 1990.
[55] D.D. Wagman, W.H. Evans, V.B. Parker, R.H. Schumm, I. Halow, S. Bailey, K.L. Churney, R.L. Nuttal, The NBS tables of chemical thermodynamic properties. Selected values for inorganic and C1 and C2 organic substances in SI units, J. Phys. Chem. Ref. Data 11 (2) (1982) 2–392.
[56] J.G. Aston, C.W. Ziemer, Thermodynamic properties of three crystalline forms of methylammonium chloride, J. Am. Chem. Soc. 68 (1946) 1405–1413.
[57] J. Timmermans, Physico-chemical Constants of Pure Organic Substances, second ed., Elsevier, New York, NY, 1965.
[58] S. Budavari (Ed.), The Merck Index, An Encyclopedia of Chemicals, Drugs, and Biologicals, Merck & Co., Rahway, NJ, 1989.
[59] W.A. Felsing, A.R. Thomas, Vapor pressures and other physical constants of methylamine and methylamine solutions, Ind. Eng. Chem. 21 (1929) 1269–1272.
[60] S. Bergström, G. Oloffson, Thermodynamic quantities for the dissociation of the methylammonium ions between 273 and 398 K, J. Chem. Thermodyn. 9 (1977) 143–152.
[61] D.H. Everett, W.F.K. Wynne-Jones, The dissociation constants of the methylammonium ions and the basic strengths of the methylamines in water, Proc. R. Soc. Lond. Ser. A Math. Phys. Sci. 177 (1941) 499–516.
[62] E. Grunwald, E. Price, Ionization and proton exchange of amines in acetic acid. I. Kinetic and equilibrium properties for solutions of methylamine, J. Am. Chem. Soc. 86 (1964) 2965–2970.
[63] W.A. Felsing, B.A. Phillips, Partial vapor pressures of aqueous methylamine solutions, J. Am. Chem. Soc. 58 (1936) 1973–1975.
[64] A.O. Christie, D.J. Crisp, Activity coefficients of the n-primary, secondary and tertiary aliphatic amines in aqueous solutions, J. Appl. Chem. 17 (1967) 11–14.
[65] A. Kisza, Physico-chemical properties of fused organic salts. Part I. Vapor pressure and heat of vaporization, Rocz. Chem. Ann. Soc. Chim. Pol. 41 (1967) 351–361.
[66] J. Błażejowski, Thermal properties of amine hydrochlorides. Part I. Thermolysis of primary n-alkylammonium chlorides, Thermochim. Acta 68 (1983) 233–261.
[67] A.G. Tereshchenko, L.A. Chemeris, The solubility of methylammonium halides in water in the range 0–80°C, Russ. J. Phys. Chem. 49 (1975), 1445–1445.
[68] E.F. Zhuravlev, M.I. Kadantseva, Sistema khlorid tseriya – khlorid metilamina – voda, Zhurnal Neorg. Khimii 16 (1971) 2867–2869.
[69] E.F. Zhuravlev, Y.N. Nasyrov, N.I. Rakhmangulova, Sovmestnaya rastvorimost' khlorida prazeodima s khloridami mono-, di- i trimetilaminov v vode, Zhurnal Neorg. Khimii 20 (1975) 1696–1700.
[70] A.B. Garrett, S.A. Woodruff, A study of several physical properties of electrolytes over the temperature range of 25°C to – 73°C, J. Phys. Chem. 55 (1951) 477–490.
[71] J.H. Jones, F.J. Spuhler, W.A. Felsing, The determination of the activity coefficients of the methylamine hydrochlorides from freezing point data, J. Am. Chem. Soc. 64 (1942) 965–968.
[72] G. Tamman, Die Dampfttensionen der Lösungen, Z. Phys. Chem. 2 (1888) 42–47.
[73] O.D. Bonner, Osmotic and activity coefficients of methyl-substituted ammonium chlorides, J. Chem. Soc. Faraday Trans. I 77 (1981) 2515–2518.
[74] J.B. Macaskill, A.D. Pethybridge, Osmotic coefficients and activity coefficients of methyl-substituted ammonium chlorides and ammonium methyl sulphates in water at 25°C, J. Chem. Soc. Faraday Trans. 71 (1975) 1465–1468.
[75] J.M. Bolling, A.R. Collett, C.L. Lazzell, Some physical properties of morpholine, Proc. W. Va. Acad. Sci. 19 (1947) 61.
[76] M. Palczewska-Tulińska, J. Choliński, A. Szafrański, D. Wyrzykowska-Stankiewicz, Isobaric vapor-liquid equilibrium in the three binary systems involving morpholine, Fluid Phase Equilib. 5 (1980) 113–129.
[77] V. Savescu, I. Ionescu, D. Cioroianu, Liquid-vapor equilibria in binary systems containing morpholine, Rev. Roum. Chim. 41 (1996) 371–380.
[78] S. Cabani, G. Conti, D. Giannessi, L. Lepori, Thermodynamic study of aqueous dilute solutions of organic compounds. Part 3. – Morpholines and piperazines, J. Chem. Soc. Faraday Trans. I (1975) 1154–1160.
[79] M.-J. Lee, C.-C. Su, H.-M. Lin, Isothermal vapor-liquid equilibria for binary mixtures composed of the closely boiling compounds 1,2-dimethoxybenzene and 2-methoxyphenol with an adducted agent: tert-butanol or morpholine, J. Chem. Eng. Data 49 (2004) 588–593.
[80] B. Marrufo, M. Sanchotello, S. Loras, Isobaric vapor–liquid equilibria for binary and ternary mixtures with cyclohexane, cyclohexene, and morpholine at 100 kPa, Fluid Phase Equilib. 296 (2010) 178–183.
[81] C. Pettenati, P. Alessi, M. Fermeglia, I. Kikic, Vapor liquid equilibrium data for systems containing morpholine, Fluid Phase Equilib. 54 (1990) 81–91.
[82] A.-M. Simoiu, A. Iacob, Thermodynamic study of the vapor–liquid equilibrium (VLE) data of the mixture formed by diethylenimide oxide with benzene, J. Therm. Anal. Calorim. 110 (2012) 329–334.
[83] A.L. Wilson, New aliphatic amines, Ind. Eng. Chem. 27 (1935) 867–871.
[84] H.S. Wu, W.E. Locke III, S.I. Sandler, Isothermal vapor-liquid equilibrium in binary mixtures containing morpholine, J. Chem. Eng. Data 36 (1991) 127–130.
[85] R.E. Mesmer, B.F. Hitch, Base strength of amines at high temperatures. Ionization of cyclohexylamine and morpholine, J. Solut. Chem. 6 (1977) 251–261.
[86] H.B. Hetzer, R.G. Bates, R.A. Robinson, Dissociation constant of morpholinium ion and related thermodynamic quantities from 0 to 50°C, J. Phys. Chem. 70 (1966) 2869–2872.
[87] M.K. Ridley, C. Xiao, D.A. Palmer, D.J. Wesolowski, Thermodynamic properties of the ionization of morpholine as a function of temperature and ionic strength, J. Chem. Eng. Data 45 (2000) 502–507.
[88] J.B. Czerminski, A.G. Dickson, R.G. Bates, Thermodynamics of the dissociation of morpholinium ion in seawater from 5 to 40°C, J. Solut. Chem. 11 (1982) 79–89.
[89] D. Fernandes, W. Conway, X.-G. Wang, R. Burns, G. Lawrance, M. Maeder, G. Puxty, Protonation constants and thermodynamic properties of amines for post combustion capture of CO_2, J. Chem. Thermodyn. 51 (2012) 97–102.
[90] H.K. Hall Jr., Field and inductive effects on the base strengths of amines, J. Am. Chem. Soc. 78 (1956) 2570–2572.
[91] Ø.B. Vistad, D.E. Akporiaye, F. Taulelle, K.P. Lillerud, Morpholine, an in situ 13C NMR pH meter for hydrothermal crystallogenesis of SAPO-34, Chem. Mater. 15 (2003) 1650–1654.
[92] A.R. Ingram, W.F. Luder, The ionization constant of morpholine in water, J. Am. Chem. Soc. 64 (1942) 3043–3044.
[93] V.L. Skorokhodova, N.V. Filippova, Y.P. Vauchsky, Issledovaniye ravnovesiya zhidkost'-par w sistemakh voda-morfolin, diglikholamin-dietilenglikhol, Zh. Prikl. Khim. Leningr. 57 (1984) 405–406.
[94] M. Sovova, T. Boublik, Liquid-vapor equilibrium. Part C. Vapor-liquid equilibrium in the water(1)-morpholine(2) system at the pressures of 50 and 75 kPa, Collect. Czech. Chem. Commun. 51 (1986) 1899–1902.
[95] D. Féron, I. Lambert, Thermal stability of three amines in pressurized water reactor secondary systems. Laboratory and loop experiments, J. Solut. Chem. 21 (1992) 919–932.
[96] O. Kiyohara, G. Perron, J.E. Desnoyers, Volumes and heat capacities of cyclic ethers and amines in water and of some electrolytes in these mixed solvents, Can. J. Chem. 53 (1975) 2591–2597.
[97] M. Al-Juaied, G.T. Rochelle, Thermodynamics and equilibrium solubility of

carbon dioxide in diglycolamine/morpholine/water, J. Chem. Eng. Data 51 (2006) 708–717.
[98] N.S. Matin, J.E. Remias, J.K. Neathery, K. Liu, The equilibrium solubility of carbon dioxide in aqueous solutions of morpholine: experimental data and thermodynamic modeling, Ind. Eng. Chem. Res. 52 (2013) 5221–5229.
[99] R.A.B. Bannard, A.A. Casselman, Paper chromatography of some amine hydrochlorides and acetates in acidic solvent systems, Can. J. Chem. 43 (1965) 395–404.
[100] P. Fearnside, C.J. Murphy, Process using amine blends to inhibit chloride corrosion in wet hydrocarbon condensing systems, United States Patent 5714664, 1998.
[101] R.K. Gaifutdinova, A.A. Sharafutdinova, Y.I. Murinov, Sistemy gidrokhlorid piridina, piperidina, piperazina, morfolina – khlorid terbiya (disproziya) – voda, Zhurnal Neorg. Khimii 33 (1988) 1060–1062.
[102] D. Venkappayya, G. Aravamudan, Phase equilibrium studies on the systems cupric chloride – morpholine chloride – water and zinc chloride – morpohline hydrochloride – water, J. Indian Chem. Soc. 58 (1981) 6–9.
[103] Huntsman, Technical Bulletin. N-Methylmorpholine (NMM), 2007.
[104] A. Belabbaci, A. Razzouk, I. Mokbel, J. Jose, L. Negadi, Isothermal vapor-liquid equilibria of (monoethanolamine + water) and (4-methylmorpholine + water) binary systems at several temperatures, J. Chem. Eng. Data 54 (2009) 2312–2316.
[105] L. Fele, P. Vidali, P. Alessi, M. Fermeglia, Recovery of N-methylmorpholine from waste aqueous streams by distillation, Chem. Eng. Sci. 69 (1994) 3677–3680.
[106] H.K. Hall Jr., Potentiometric determination of the base strength of amines in non-protolytic solvents, J. Phys. Chem. 60 (1956) 63–70.
[107] S. Xu, F.D. Otto, A.E. Mather, Dissociation constants of some alkanolamines, Can. J. Chem. 71 (1993) 1048–1050.
[108] S. Cabani, V. Mollica, L. Lepori, S.T. Lobo, Volume changes in the proton ionization of amines in water. 1. Morpholines and piperazines, J. Phys. Chem. 81 (1977) 982–987.
[109] M.J. Blais, O. Enea, G. Berthon, Étude thermodynamique de la protonation de la morpholine et certains de ses dérivés, Thermochim. Acta 12 (1975) 25–28.
[110] L. Knorr, Synthesen in der "Oxazinreihe", Ber. Dtsch. Chem. Ges. Berl. 22 (1889) 2081–2099.
[111] N. Chiali-Baba-Ahmed, F. Dergal, L. Negadi, I. Mokbel, Measurement and correlation of the (vapor + liquid) equilibria of pure 4-ethylmorpholine, 1,2-dimethylisopropylamine and N,N-dimethylethanolamine, and their binary aqueous solutions, J. Chem. Thermodyn. 63 (2013) 44–51.
[112] Huntsman, Technical Bulletin. N-Ethylmorpholine (NEM), 2007-2008.
[113] R.N. Goldberg, N. Kishore, R.M. Lennen, Thermodynamic quantities for the ionization reactions of buffers, J. Phys. Chem. Ref. Data 31 (2002) 231–370.
[114] Z.M. Anwar, Y.K. Sung, Synthesis and solution properties of La(III)-N-ethylmorpholine complex, Bull. Korean Chem. Soc. 26 (2005) 614–618.
[115] G. Ovejero, M.D. Romero, E. Díez, I. Díaz, P. Pérez, Thermodynamic modeling and simulation of styrene – butadiene rubbers (SBR) solvent equilibrium staged processes, Ind. Eng. Chem. Res. 48 (2009) 7713–7723.
[116] J.W. Cobble, P.J. Turner, Additives for PH Control in PWR Secondary Water, Report EPRI NP-4209, Electric Power Research Institute, Palo Alto, CA, 1985.